

Biocatalytic Carboxylation of Phenol Derivatives:  
Kinetics and Thermodynamics of the Biological Kolbe-Schmitt  
Synthesis

*L. Pesci,<sup>1</sup> S. M. Glueck,<sup>2,3</sup> P. Gurikov,<sup>4</sup> I. Smirnova,<sup>4</sup> K. Faber,<sup>3</sup> A. Liese<sup>1</sup>*

<sup>1</sup> Institute of Technical Biocatalysis, Hamburg University of Technology, Germany

<sup>2</sup> ACIB GmbH c/o

<sup>3</sup> Department of Chemistry, Organic & Bioorganic Chemistry, University of Graz, Austria

<sup>4</sup> Institute of Thermal Separation Processes, Hamburg University of Technology, Germany

Corresponding author: Andreas Liese, Institute of Technical Biocatalysis, Hamburg University of Technology, Germany, Tel: +49-40-42878-3018, Fax: +49-40-42878-212, email: liese@tuhh.de

Article type : Original Article

## ABSTRACT

Microbial decarboxylases, which catalyze the reversible regio-selective *ortho*-carboxylation of phenolic derivatives in anaerobic detoxification pathways, have been studied for their reverse carboxylation activities on electron-rich aromatic substrates. *Ortho*-hydroxybenzoic acids are important building blocks in the chemical and pharmaceutical industries and are currently produced *via* the Kolbe-Schmitt process, which requires elevated pressures and temperatures ( $\geq 5$  bar,  $\geq 100$  °C) and often shows incomplete regio-selectivities. In order to resolve bottlenecks in view of preparative scale applications, we studied the kinetic parameters for 2,6-dihydroxybenzoic acid decarboxylase from *Rhizobium* sp. in the carboxylation- and decarboxylation-direction using 1,2-dihydroxybenzene (catechol) as starting material. The catalytic properties ( $K_m$ ,  $V_{max}$ ) are correlated with the overall thermodynamic equilibrium *via* the Haldane equation, according to a reversible random bi-uni mechanism. The model was subsequently verified by comparing experimental results with simulations. This work provides insights into the catalytic behavior of a non-oxidative aromatic decarboxylase and reveals key limitations (*e.g.*, substrate oxidation, CO<sub>2</sub> pressure,

This article has been accepted for publication and undergone full peer review but has not been through the copyediting, typesetting, pagination and proofreading process, which may lead to differences between this version and the Version of Record. Please cite this article as doi: 10.1111/febs.13225

This article is protected by copyright. All rights reserved.

enzyme deactivation, low turnover frequency) in view of the employment of this system as a 'green' alternative to the Kolbe-Schmitt processes.

**Keywords:** Kolbe-Schmitt reaction, biocatalytic carboxylation, non-oxidative carboxylation, enzyme deactivation, kinetic modelling, thermodynamics.

## INTRODUCTION

The Kolbe-Schmitt process for the carboxylation of hydroxy-aromatics is known since about a century and allows access to carboxylic acids on industrial scale by employing carbon dioxide as a C1 building block for organic synthesis [1]. The original process has been customized to the type of substrate and the reaction conditions [2, 3]. In general, the reaction suffers from equilibrium-limited yields of about 60% and from incomplete regio-selectivities regarding *o,p*-isomeric products and requires harsh conditions in terms of pressure (50-100 bar) and temperature (100-200 °C). Less reactive mono-phenols need anhydrous reaction conditions [3]. Recently, new investigations have been carried out to optimize these processes by use of different reaction media, such as “reactive” ionic liquids based on bicarbonate as anion, microwave-based heating and flow operation modes [4, 5]. On the other hand, a biological equivalent to the Kolbe-Schmitt reaction has been discovered in the microbial anaerobic detoxification of phenolic compounds, where non-oxidative decarboxylases act in the C-C bond forming direction [6–8] to furnish a more polar and water soluble carboxylate anion [9, 10]. As usual in biodegradation, the substrate promiscuity is high [11, 12]. In line with the mechanism of electrophilic aromatic substitution ( $S_EAr$ ), two types of selectivities were found in the biological carboxylation of phenolic substrates: *ortho* and *para* carboxylation.

*Ortho*-selectivity is displayed by hydroxybenzoic and salicylic acid decarboxylases [13, 14]. These well investigated enzymes share common features, such as exclusive regio-selectivity and absence of cofactors. Even with electron-rich substrates, conversions are limited to a range of 10 to 40%, which is partly ascribable to the reaction equilibria. Higher carboxylation yields are achieved in the presence of elevated bicarbonate concentrations (usually ~3M) [11, 15, 16]. 2,6-Dihydroxybenzoic acid decarboxylases (or  $\gamma$ -resorcylic acid decarboxylases) were described from *Rhizobium* sp. and *Pandoraea* sp. [13, 17]. Ample information is available on the substrate tolerance and the crystal structure revealing a catalytically essential  $Zn^{2+}$ , which allowed the proposal for a reaction mechanism [12, 18]. Preliminary studies on the influence of reaction conditions on the catalytic performance revealed that the presence

water-miscible organic solvents and ionic liquids as alternative reaction media increased the yields in resorcinol carboxylation from 30% up to 50% [8]. Despite this broad knowledge, only poor kinetic information is available, i.e.  $K_m$  values of 25.9 mM for resorcinol and 0.08 mM for its carboxylated product, and a  $K_m$  of 0.12 mM for 2,3-dihydroxybenzoate [17].

In this work, we present our investigations on enzyme kinetics together with the reaction thermodynamics in line with the verification of the catalytic mechanism of 2,6-dihydroxybenzoic acid decarboxylase (DHBA decarboxylase) from *Rhizobium* sp. with catechol as the phenolic substrate (Scheme 1). This study elucidates intrinsic bottlenecks for the design of biochemical carboxylation processes of phenolic compounds.

## RESULTS

**Reaction medium and substrate oxidation.** Usually, the carboxylation activity for non-oxidative decarboxylases is tested using  $\text{KHCO}_3$  close to saturating concentrations ( $\sim 3\text{M}$ ) in 100 mM potassium phosphate ( $\text{KP}_i$ ) buffer. High bicarbonate concentrations are necessary to drive substrate conversion due to a Le Chatelier effect, while the  $\text{KP}_i$  buffer is reported to compensate for the pH increase due to the addition of bicarbonate [19, 16, 11].

Considering the equilibrium constants at  $25^\circ\text{C}$  for the dissociation of carbonic acid to bicarbonate anion, it can be calculated, that regardless of the salt concentration, the pH of such a solution would be 8.3. Consequently, due to the high concentration, it is not likely to expect any pH shift as a consequence of carboxylate formation, which can reach concentrations of  $\leq 20$  mM. Unless phosphate exhibits a positive effect on the enzyme activity, one would not expect any differences in activity and long term conversion in  $\text{KHCO}_3$  solution (2 M),  $\text{KHCO}_3/\text{K}_2\text{CO}_3$  buffer (2M),  $\text{KHCO}_3$  (2M) in  $\text{KP}_i$  buffer 0.1 M pH 5.5 (Figure S1). The long term-conversions ranged in all cases between 26 and 28%, indicating that there is no appreciable effect of the  $\text{KP}_i$  buffer on the enzyme stability or the reaction thermodynamics. Consequently, the following experiments were performed using an unbuffered bicarbonate solution.

In order to evaluate possible chemical oxidation of the substrate, progress curves were obtained by performing the reaction in an open and a closed reaction vessel. After around 3 hours, the product concentration reached a constant value of approximately 2.6 mM, while catechol continued to be consumed. The progress curves clearly indicate that the substrate is oxidized by air yielding the reactive *o*-quinone, which in turn polymerizes going in hand with a color change of the solution from light brown to black (Figure S2). The same phenomenon was observed with purified DHBA decarboxylase, which excludes the undesired action of

oxidases (such as Cu-dependent monooxygenases) present in crude CFE [20]. In order to circumvent any competing chemical substrate oxidation, we tested several parameters (such as addition of a reductant, solution degassing, protection from light) and we found the addition of stoichiometric amounts of ascorbic acid as an effective tool to suppress the chemical formation of quinone by autooxidation (Scheme S1 and Figure S3).

**Kinetics.** The carboxylation requires two substrates (catechol and bicarbonate) with the formation of one product, 2,3-dihydroxybenzoic acid (DHBA), according to a bi-uni reaction. As a consequence, kinetic analyses need to be conducted with purified enzyme on both substrates (maintaining the other in saturating amounts), and on the product (due to the reversibility of the reaction) in order to elucidate the specific activity and to calculate the turnover frequency. Figure 1 shows initial rate measurements for catechol. The presence of constant amounts of co-substrate bicarbonate (2 M, corresponding to 2.3 times its  $K_m$ ) was ensured by keeping the conversion below 10 %. With limited enzyme amounts (0.20-0.30 mg/mL) the reaction was slow enough to measure initial rates directly, taking samples during the first 20 minutes of the reaction, where zero order kinetics still occurs.

The profile shows a typical hyperbolic behavior up to 120 mM, whereas the reaction rate steeply decreases beyond this value. This trend is not ascribable to substrate surplus inhibition, where a second substrate molecule behaves as uncompetitive inhibitor, as it was impossible to fit the experimental points with the corresponding equation. Experimental points in the concentration range of 0-120 mM were fitted using the double substrate Michaelis-Menten equation. From this plot, a  $K_m$  for catechol ( $K_{m,c}$ ) of  $30 \pm 3$  mM and a  $V_{max}^f$  in the carboxylation direction of  $0.35 \pm 0.01 \mu\text{mol min}^{-1} \text{mg}^{-1}$  of decarboxylase can be calculated. In the literature a  $K_m$  of 25.9 mM is known for a 2,6-dihydroxybenzoic acid decarboxylase from *Agrobacterium tumefaciens* using 1,3-dihydroxybenzene (resorcinol) as substrate [17]. Previous studies on non-oxidative aromatic bio-carboxylation reveal that the maximum conversion is higher at relatively low substrate concentrations, depending on the enzyme type and the substrate. For example, in the *ortho*-carboxylation of 5-methyl-1,3-dihydroxybenzene (orcinol) and resorcinol catalyzed by DHBA decarboxylase, conversions drop from 67 and 35% at 10 to 50 mM substrate concentrations to 4 and 15% at approximately 200 mM substrate concentrations, respectively [18, 8]. The same behavior was found in the *o*-carboxylation of *p*-aminophenol yielding *p*-aminosalicylic acid, where the maximal conversion dropped from 70% at 10 mM to 20% at 200 mM [21]. The same trend

was observed with hetero-aromatics (pyrrole to pyrrole-2-carboxylate) [19]. Although these findings are generally explained by substrate inhibition, our kinetic plot for catechol does not fit to this hypothesis. The drastic drop in reaction rate could better be explained by enzyme deactivation at elevated substrate concentration. To verify this hypothesis, we performed a deactivation test developed by M. J. Selwyn in 1954 [22]. The test is based on the fact that in absence of enzyme deactivation, product formation over time is only a function of time and enzyme concentration, if all the other parameters are kept constant. It follows that performing enzymatic reactions with different enzyme amounts and plotting product concentration vs. time multiplied by enzyme concentration, the points must coincide with the same curve. If denaturation occurs, the enzyme amount itself becomes a function of time, and different curves will be obtained. Figure 2 shows the results of the deactivation test at substrate concentrations of 30 and 200 mM.

Reaction progress clearly shows that at high substrate concentrations the enzyme concentration is not constant anymore, since higher conversions were obtained with higher enzyme amounts. Recently, Ienaga *et al.* have shown that replacement of Tyr 64 and Phe 195 (corresponding to Asn60 and Phe 189 in 2,6-dihydroxybenzoic acid decarboxylase from *Rhizobium* sp.) by Thr and Tyr, respectively, around the active site of salicylic acid decarboxylase from *T. moniliiforme* yields a mutant which reached the same maximal conversion of *p*-aminosalicylic acid (70%) within a range of 10 to 200 mM of substrate [21]. This shows how key amino acid residues may be substituted resulting in enhanced protein stabilization, possibly as a consequence of the introduction of additional OH groups (Thr64 and Tyr195). To assess the kinetic behavior with regard to bicarbonate, 100 mM of catechol was used at saturating concentration (3.3 times  $K_{m,c}$ ) and the co-substrate concentration was varied from 0 to 3 M (approx. saturation). Figure 3 shows the double substrate Michaelis-Menten fit.

The non-linear fit revealed a  $K_m$  for bicarbonate ( $K_{m,b}$ ) equal to  $839 \pm 4$ . From the typical rectangular hyperbola it can be concluded that enzyme kinetics are not significantly affected by different ionic strength values. Complete evaluation of the enzyme kinetics requires the catalytic properties in the reverse decarboxylation direction. Since in this case, bicarbonate cannot be introduced, it was decided to buffer the system at pH 8 (the same value as in the forward carboxylation direction) to counteract the pH shift due to the acidic substrate. Since the reaction rate in the (downhill) decarboxylation direction was significantly higher as

compared to the (uphill) carboxylation direction, in a 20 minutes assay it was possible to generate progress curves of the reaction, from which initial rates were derived. The one-substrate kinetic fit is shown in Figure 4.

The catalytic constants  $K_{m,HA}$  and  $V_{max}^r$  for the decarboxylation reaction were  $1.2 \pm 0.3$  mM and  $1 \pm 0.1$   $\mu\text{mol min}^{-1} \text{mg}^{-1}$ . The catalytic parameters  $K_m$ ,  $V_{max}$ ,  $k_{cat}$  and the specificity constant  $K_a$  are summarized in Table 1.

In general, the enzyme appears more efficient in catalyzing the decarboxylation reaction, as shown by the  $K_a^{HA}$ , the combination of  $K_{m,HA}$  and  $k_{cat}$ . As previously assumed, the presence of the lower  $V_{max}^f$  is the result of the thermodynamically more difficult 'uphill' C-C bond formation compared to the cleavage [19].

**Activation Energy.** The completion of the kinetic study requires the determination of the activation energy of the rate limiting step in the overall mechanism. The maximum reaction rate was measured at 20, 30, 40 and 50° C, which was accompanied by an increase in carboxylation activities. The Arrhenius equation was used to calculate the activation energy (Figure S4), which resulted in  $29 \pm 0.2$  kJ mol<sup>-1</sup> ( $7.00 \pm 0.06$  kcal mol<sup>-1</sup>). It is interesting to note that from theoretical studies on the Kolbe-Schmitt reaction for phenol carboxylation, similar activation energies of 5.4 and 10.3 kcal mol<sup>-1</sup> were calculated for the nucleophilic attack of the phenolate anion to the electrophilic carbon atom of CO<sub>2</sub> [24]. The close similarity of the  $E_a$  of the chemical and the biological carboxylation further supports the strong mechanistic relationship of benzoic acid decarboxylases with the Kolbe-Schmitt reaction [12].

**Thermodynamics.** Determination of the equilibrium point, controlled by thermodynamics, can be hampered by product inhibition and enzyme deactivation. Thus, long-term experiments were performed using non-limiting enzyme amounts and varying the concentration of the two substrates. In the absence of product inhibition or enzyme deactivation, a linear correlation of maximal conversion is expected by increasing the substrate (catechol) concentration at fixed bicarbonate concentration. Conversely, higher conversion is expected at increasing bicarbonate concentration, while maintaining a fixed substrate concentration. The enzyme concentrations employed in these set of experiments ensured the occurrence of steady state concentrations after few hours of reaction. The results

are in accordance with previously reported trends from similar systems [16, 8, 19] and are depicted in Figs. 5 and 8.

Figure 5 shows that a steady maximal conversion of approximately 23 % is obtained at 10 to 80 mM substrate concentration, where deactivation effects are negligible. In this range, it can be assumed that the maximal conversion corresponds to the equilibrium conversion. Beyond this threshold, the conversion drastically drops due to enzyme deactivation (Figure 2) and the value is therefore depending on the enzyme concentration. For the converse experiment, a fixed 10 mM concentration of catechol was used to measure the equilibrium shift at increased amounts of bicarbonate. From the law of mass balance, the equilibrium constant for the carboxylation was calculated to be  $1.6 \cdot 10^{-4} \pm 8.0 \cdot 10^{-6} \text{ M}^{-1}$ . From this, it is possible to calculate the difference in standard free energy at 303 K using the Van't Hoff isotherm equation:  $\Delta G^0 = 5.2 \pm 0.03 \text{ kcal mol}^{-1}$ .

**Carboxylation under CO<sub>2</sub> pressure.** The biocatalytic carboxylation of phenolics and hetero-aromatics under CO<sub>2</sub> pressure (even supercritical conditions) was reported [13, 25]. To study the influence of gaseous CO<sub>2</sub> on the enzyme, long-term experiments were undertaken at pressures of 50 and 80 bar. To ensure the supercritical state of the gas at 80 bar, tests were performed at 40°C. Additional tests were performed to exclude temperature effects on enzyme stability and thermodynamics, as well as pH. Although water pressurized with CO<sub>2</sub> at >30 bar has a pH of 3 at room temperature [26], we found a drop of only 0.5 – 1 pH units for both KP<sub>i</sub> and bicarbonate buffers pressurized by CO<sub>2</sub>. Hence, KP<sub>i</sub> buffer (0.2 M, pH 8.0) was used to balance the pH decrease caused by CO<sub>2</sub> dissolution in the reaction media. The results are shown in Table 2.

Close to the limits of accuracy, conversions of 5-7 % were found at 50 and 80 bar, indicating no significant influence of dissolved CO<sub>2</sub> concentration on the conversion. In contrast, a conversion of 25% was achievable only in the presence of 2 M KHCO<sub>3</sub> under a gas pressure of 80 bar. According to literature data, the amount of dissolved carbon dioxide levels off at a pressure of ~100 bar, which corresponds to ~1.2 M solution and at 50 and 80 bar, the solubility of CO<sub>2</sub> is 0.87 M and 1.1 M, respectively [27, 28], giving approximately half of the bicarbonate concentration used in unpressurized experiments. Taking the pH of the pressurized solution into account, the bicarbonate concentration can be estimated as 4 mM, which is considerably lower than the corresponding KHCO<sub>3</sub> concentration used at ambient



conditions (from 0.1 to 3 M). These data underline that for 2,6-DHBA decarboxylase from *Rhizobium* the co-substrate is bicarbonate rather than (dissolved) CO<sub>2</sub>. From literature data, it seems that the ability to use CO<sub>2</sub> is strongly dependent on the enzyme type, even though they accept similar substrates and share similar biological role.

For instance, Mn<sup>2+</sup>-dependent phenol carboxylase from *Thauera aromatica* catalyzes the *para*-carboxylation of phenyl phosphate under CO<sub>2</sub> atmosphere (1 bar) in the presence of 100 mM of NaHCO<sub>3</sub> [7]. Likewise, metal-independent pyrrole-2-carboxylate decarboxylase from *B. megaterium* exhibited a higher reaction rate and conversion in the presence of 3 M KHCO<sub>3</sub> with a bell-shaped dependency on CO<sub>2</sub> pressure [25], although the enzyme uses HCO<sub>3</sub><sup>-</sup> as the reactive species [19]. In contrast, the behavior of 2,6-DHBA decarboxylase from *Rhizobium* is similar to that of 2,6-dihydroxybenzoic acid decarboxylase from *Pandorea* sp. acting on resorcinol, where the conversion decreased in presence of KHCO<sub>3</sub> under supercritical CO<sub>2</sub> pressure [13]. Influence of moderate pressure on enzymatic reactions is versatile and may lead either to inhibitory effects or extra activation [29, 30]. In addition, drastic effects can be observed in presence of organic (co)solvents, which strongly manipulate CO<sub>2</sub> solubility [8]. The direct use of gaseous CO<sub>2</sub> in biocatalytic carboxylation is currently being studied.

**Modelling.** The development and validation of a kinetic model for an enzymatic reaction allows to verify the quality of the determined catalytic constants. Since the carboxylation using bicarbonate as co-substrate consists of a formal addition of two substrates, selectively binding to two different sites, forming a single product followed by water elimination, a bi-uni mechanism is proposed. The proposed mechanism for DHBA decarboxylase assumes binding of bicarbonate by Zn<sup>2+</sup> and the phenolic substrate by Asp 287 [12, 18]. Macroscopically the sequence of binding is not fixed and therefore we rather assume a random mechanism; ordered binding being more typical for external cofactors-dependent enzymes (e.g., NADH/NADPH-dependent reductions), where usually the coenzyme binds first [31, 32]. Assuming that the C-C bond formation during the conversion of the ternary enzyme-two-substrates complex to the enzyme-product complex is the rate-limiting step, while other binding events are in rapid equilibrium, the following catalytic mechanism (Figure 6) and kinetic equation (Equation 1) can be drawn:



$$\frac{d[HA]}{dt} = [E] v = [E] \frac{\frac{V_{max}^f}{K_m^c K_c^b} [C] [B] - V_{max}^r \frac{[HA]}{K_{m,HA}}}{1 + \frac{[C]}{K_m^c} + \frac{[B]}{K_m^b} + \frac{[HA]}{K_{m,HA}} + [C] \frac{[B]}{K_m^c + K_c^b}} \quad (1)$$

The only unknown parameter in the equation is the dissociation constant of the ternary complex ( $K_c^b$ ). At reaction equilibrium, the net reaction velocity equals zero, where the law of mass action is related to the catalytic constants by the Haldane equation (Equation 2).

$$K_{eq} = \frac{[HA]_{eq}}{[C]_{eq} [B]_{eq}} = \frac{V_{max}^f K_{m,HA}}{V_{max}^r K_c^b K_m^c} \quad (2)$$

From equation 2, the dissociation constant can be calculated as  $K_c^b = 87$  mM. The solutions of the differential equation are compared with the experimental results obtained at different reaction conditions (Figure 7).

The good agreement between experimental and theoretical values supports the proposed kinetic mechanism as a viable model for the biocatalytic carboxylation. Moreover, as shown in Figure 8, also the equilibrium positions can be modeled and predicted with very good agreement.

## DISCUSSION

The reversible regioselective carboxylation of catechol catalyzed by 2,6-dihydroxybenzoic acid decarboxylase from *Rhizobium* sp. has been kinetically characterized and the kinetic properties of the enzyme have been linked to the overall thermodynamic equilibrium, which further strengthened the proposed mechanism (Scheme 2).

In comparison, related (de)carboxylases, such as pyrrole-2-carboxylate decarboxylase from *Bacillus megaterium* shows a  $K_m$  of 61 mM for its substrate pyrrole, a  $K_m$  of 560 mM for the co-substrate bicarbonate and a  $V_{max}$  in the forward (carboxylation) direction of 47.2  $\mu\text{mol min}^{-1} \text{mg}^{-1}$  [19]. In a related fashion, salicylic acid decarboxylase from *T. moniliiforme* shows  $K_m$  and  $V_{max}$  of 123 mM and 1.23  $10^{-2} \mu\text{mol min}^{-1} \text{mg}^{-1}$  for phenol as substrate and a  $K_m$  and  $V_{max}$  of 1.08 mM and 0.47  $\mu\text{mol min}^{-1} \text{mg}^{-1}$  in the reverse direction for the *o*-carboxylation product [16]. For 2,3-dihydroxybenzoic acid decarboxylase from *Aspergillus oryzae*,  $K_m$  and

*Accepted Article*

$V_{\max}$  values for 2,3-dihydroxybenzoic acid were 0.42 mM and 4.8  $\mu\text{mol min}^{-1} \text{mg}^{-1}$  [33]. Our results from 2,6-dihydroxybenzoic acid decarboxylase from *Rhizobium* sp. are in accordance with these values, as higher  $V_{\max}$  and lower  $K_m$  values were generally found in the more favorable 'downhill' direction. The fact, that irrespective of the type of phenolic or hetero-aromatic substrates, the catalytic constants are approximately in the same order of magnitude, even among different enzymes sources, is an example how catalytic constants evolved up to the thermodynamic limit. This connection between catalytic parameters and thermodynamic equilibrium has been pointed out by I. Segel in 1983 [34] and for this enzyme class, it can be assumed that evolutionary events have tended to maximize the carboxylation efficiency by increasing  $V_{\max}$  and decreasing  $K_m$  for the carboxylates, in order to leave the equilibrium constants unchanged. The relationship between the catalytic parameters of an enzyme and the thermodynamic equilibrium (equation 2) is meaningful only when the chemical equilibrium is reached and in the case of the biocatalytic carboxylation this seems the case at relatively low substrate concentrations, where no deactivation is present. The fact that conversions do not exceed 7% under  $\text{CO}_2$  pressure of 50 or 80 bar can be translated into an infinite  $K_m$  for the binding of (neutral) carbon dioxide to the enzyme and the low conversion under  $\text{CO}_2$  pressure is the result of the slow equilibrium between  $\text{CO}_2$  and bicarbonate. In contrast, the latter clearly appears to be the co-substrate, which is favorably bound to the catalytically essential  $\text{Zn}^{2+}$  ion in the active site. The preference of the enzyme for bicarbonate as co-substrate (rather than  $\text{CO}_2$ ) can be explained by its higher availability in water.

The mechanism of enzymatic carboxylation shows a strong resemblance to that of the Kolbe-Schmitt reaction (Scheme 2, A and B). Although the mechanism of the latter is still not fully understood, it is generally accepted that the first step involves formation of a complex between the reactants (phenolate anion and  $\text{CO}_2$ ), linked by the positively charged metal (A) [24, 35]. This arrangement makes  $\text{CO}_2$  more electrophilic and puts it in position for nucleophilic attack, and nicely explains the regioselectivity through a 'chelate-effect': *ortho* in case of small  $\text{Na}^+$ , *para* with large  $\text{K}^+$  [36, 37]. The formation of a phenyl hemicarbonate salt as intermediate (not shown) fails to explain *para*-selectivity and is therefore less likely. C-C Bond formation occurs via classic electrophilic aromatic substitution ( $\text{Ar-S}_E$ ) through a resonance-stabilized non-aromatic intermediate, which finally regains aromaticity via tautomerization. In contrast, in the biocatalytic equivalent (B), bicarbonate serves as  $\text{CO}_2$  source, which is electronically activated by a divalent  $\text{Zn}^{2+}$  atom serving as Lewis acid to make it amenable to nucleophilic attack by catechol, which is deprotonated by Asp 287 (assisted by His 218 and Glu 221) to enhance its electron density. The (postulated) non-

aromatic oxyanion intermediate regains aromaticity via elimination of H<sub>2</sub>O and concomitant tautomerization in a similar fashion as the chemical variant [18].

## CONCLUSIONS

The kinetics and thermodynamics of the reversible non-oxidative carboxylation of catechol to 2,3-dihydroxybenzoic acid catalyzed by 2,6-dihydroxybenzoic acid decarboxylase from *Rhizobium* sp. were studied and a model based on a reversible random bi-uni mechanism was proposed, which shows good correlation between experimental and theoretical values. In view of the application of this regio-specific biocatalytic variant of the Kolbe-Schmitt process, the following key limitations were identified: (i) limited conversions obtained at high substrate concentrations were due to enzyme deactivation (rather than thermodynamic limitations), (ii) instability of the phenolic substrate due to spontaneous air-oxidation and (iii) unfavorable catalytic parameters.

In order to shift the unfavorable equilibrium into the 'uphill' (carboxylation) direction, reaction engineering techniques are currently being developed towards the design of a processes which makes use of CO<sub>2</sub> as waste gas as C1 building block for the carboxylation of phenol derivatives.

## MATERIALS AND METHODS

**General.** All chemicals were purchased from Sigma Aldrich (Buchs, Switzerland). Concentrations of substrate and product were determined by HPLC with UV detection using calibration curves obtained with authentic reference material. Activity measurements were performed by measuring five to six product/substrate concentration values in the appropriate time range. All kinetic and thermodynamic measurements were conducted in duplicate. Non-linear regression curve fits were performed minimizing the sum of the squares for the double substrate Michaelis Menten model using Microsoft Excel (Excel 2010, Microsoft). Mathematical solutions for the kinetic model were obtained using the ODE45 solver in Matlab (Matlab 2010, Mathworks).

**Overexpression and preparation of 2,6-dihydroxybenzoate decarboxylase.** Chemically competent *Escherichia coli* BL21(DE3) cells were transformed with the plasmidic vector pET21a (+) containing the His-tagged DHBA decarboxylase gene from *Rhizobium* sp. and heterologous expression was performed as previously reported [8]. For the preparation of

cell-free extracts (CFEs), wet cells (0.6 g/mL) were suspended in potassium phosphate (KPi) buffer (50 mM, pH 7.0), the suspension was sonicated (5 mm sonication tip, 70 % power, 50% duty cycle, 3 min) on ice for three times and centrifuged at 25000 rpm (75,465 g) for 30 min at 4°C. Enzyme purification was carried out using a Nickel-NTA-agarose packed column (9 cm high, conical 0.8 x 4 cm). After washing the column with equilibration buffer (Tris 20 mM, NaCl 300 mM, imidazole 10 mM, pH 7.4) with 5 column volumes, the cell free extract was loaded by gravity using a ratio of 0.5 mL of CFE per mL of chromatographic matrix. Unspecific adsorbed proteins were removed by washing with 10 column volumes with washing buffer (Tris 20 mM, NaCl 300 mM, imidazole 20 mM, pH 7.4), DHBA decarboxylase was eluted using 5 column volumes of elution buffer (Tris 20 mM, NaCl 300 mM, imidazole 250 mM, pH 7.4). All purification steps were carried out at 4°C. Imidazole was removed by ultrafiltration using exchange buffer (KPi buffer, 50 mM, pH 7.0) for storage. The biocatalyst was used either as purified enzyme or CFE.

**General procedures for the enzymatic transformations.** If not specified differently, carboxylation reactions were carried out in HPLC screw capped glass vials using an unbuffered potassium bicarbonate solution (pH 8, total volume 1 mL) with shaking at 30°C and 500 rpm. After addition of potassium bicarbonate, ascorbic acid and catechol in the desired concentration, the reactions were started by the addition of DHBA decarboxylase in the appropriate amount. Data points were taken by diluting samples (50 µL) with a water-acetonitrile solution (20:80, 450 µL) supplemented with trifluoroacetic acid (3% v/v) to stop the reaction. The samples were centrifuged (5 min, 13000 rpm 15,870 g) and analyzed by RP-HPLC. Decarboxylation reactions were performed under the same conditions apart from using KPi buffer 0.1 M, pH 8.0 as the reaction medium.

**Enzymatic transformation under pressurized CO<sub>2</sub>.** Desired amounts of catechol, ascorbic acid and decarboxylase CFE were mixed in KPi (0.2 M buffer, pH 8.0) in a teflon test tube, which was mounted to a Berghof RHS 295 high pressure autoclave equipped with heating jacket, digital manometer and magnetic stirring, while the temperature was directly controlled by a thermocouple. The autoclave was sealed and heated to 40 ±1 °C and carbon dioxide preheated to 40 °C was slowly introduced to reach the target pressure. Once the desired pressure and temperature were reached, stirring was turned on (500 rpm) and these conditions were kept constant for 24 h. Then, the pressure was slowly released (5 bar/min) and the temperature was lowered to room conditions.

**Analytical methods.** Catechol and 2,3-dihydroxybenzoic acid concentrations were measured by an Agilent LC-1100 HPLC equipped with a diode array detector using an RP Phenomenex Luna C18 column (150 x 4.60 mm, 5  $\mu$ m) at 25°C. Water/trifluoroacetic acid (0.1 %) and acetonitrile/trifluoroacetic acid (0.1 %) with a flow rate of 1 mL min<sup>-1</sup> with a gradient (0-2 min 15%; 2-10 min 15-100%; 10-12 min 100%; 12-16 min 100-15%) were used. Catechol and 2,3-dihydroxybenzoic acid were detected at 254 nm. Retention times were 6.2 min for catechol and 6.8 min for 2,3-dihydroxybenzoic acid.

## ACKNOWLEDGEMENTS

This work has been supported in part by the Austrian BMWFJ, BMVIT, SFG, Standortagentur Tirol and ZIT through the FFG-COMET funding program.

## ACKNOWLEDGEMENTS AUTHOR CONTRIBUTIONS

LP participated in planning the experiments, performed the experiments, analyzed the data and wrote the paper. PG participated in planning and realization of the experiments under carbon dioxide pressure and reviewed the paper. IS participated in planning the experiments under carbon dioxide pressure and reviewed the paper. SG and KF provided the plasmidic vector, participated in planning the experiments and wrote the paper. AL participated in planning the experiments, analyzed the data and wrote the paper.

## REFERENCES

1. Schmitt R (1885). Beitrag zur Kenntnis der Kolbe'schen Salicylsäure Synthese. *J. Prakt. Chem.* **31**, 397–411.
2. Baine O, Adamson G F, Barton J W, Fitch J L, Swayampati D R & Jeskey H (1954). A study of the Kolbe-Schmitt reaction. II. The carbonation of phenols. *J. Org. Chem.* **19**, 510–514.
3. Lindsey A & Jeskey H (1957). The Kolbe-Schmitt reaction. *Chem. Rev.* **57**, 583–620.
4. Stark A, Huebschmann S, Sellin M, Kralisch D, Trotzki R & Ondruschka B (2009). Microwave-Assisted Kolbe-Schmitt Synthesis Using Ionic Liquids or Dimcarb as Reactive Solvents. *Chem. Eng. Technol.* **32**, 1730–1738.

5. Hessel V, Krtischil U, Hessel V, Reinhard D & Stark A (2009). Flow Chemistry of the Kolbe-Schmitt Synthesis from Resorcinol: Process Intensification by Alternative Solvents, New Reagents and Advanced Reactor Engineering. *Chem. Eng. Technol.* **32**, 1774–1789.
6. Lack A & Fuchs G (1992). Carboxylation of phenylphosphate by phenol carboxylase, an enzyme system of anaerobic phenol metabolism. *J. Bacteriol.* **174**, 3629–3636.
7. Aresta M, Quaranta E, Liberio R, Dileo C & Tommasi I (1998) Enzymatic synthesis of 4-OH-benzoic acid from phenol and CO<sub>2</sub>: the first example of a biotechnological application of a Carboxylase enzyme. *Tetrahedron* **54**, 8841–8846.
8. Wuensch C, Schmidt N, Gross J, Grischek B, Glueck SM & Faber K (2013). Pushing the equilibrium of regio-complementary carboxylation of phenols and hydroxystyrene derivatives. *J. Biotechnol.* **168**, 264–270.
9. Brackmann R & Fuchs G (1993). Enzymes of anaerobic metabolism of phenolic compounds. *Eur. J. Biochem.* **213**, 563–571.
10. Zhang X & Young LY (1997). Carboxylation as an initial reaction in the anaerobic metabolism of naphthalene and phenanthrene by sulfidogenic consortia. *Appl. Environ. Microbiol.* **63**, 4759–4764.
11. Wuensch C, Glueck SM, Gross J, Koszelewski D, Schober M & Faber K (2012). Regioselective Enzymatic Carboxylation of Phenols and Hydroxystyrene Derivatives. *Org. Lett.* **14**, 1974–1977.
12. Goto M, Hayashi H, Miyahara I, Hirotsu K, Yoshida M & Oikawa T (2006). Crystal Structures of Nonoxidative Zinc-dependent 2,6-Dihydroxybenzoate ( $\gamma$ -Resorcyate) Decarboxylase from *Rhizobium* sp. Strain MTP-10005. *J. Biol. Chem.* **281**, 34365–34373.
13. Matsui T, Yoshida T, Yoshimura T & Nagasawa T (2006). Regioselective carboxylation of 1,3-dihydroxybenzene by 2,6-dihydroxybenzoate decarboxylase of *Pandoraea* sp. 12B-2. *Appl. Microbiol. Biotechnol.* **73**, 95–102.
14. Yoshida M, Fukuhara N & Oikawa T (2004). Thermophilic, Reversible  $\gamma$ -Resorcyate Decarboxylase from *Rhizobium* sp. Strain MTP-10005: Purification, Molecular Characterization, and Expression. *J. Bacteriol.* **186**, 6855–6863.
15. Santha R, Savithri HS, Rao A & Vaidyanathan CS (1995). 2,3-Dihydroxybenzoic Acid Decarboxylase from *Aspergillus niger*. A novel decarboxylase. *Eur. J. Biochem.* **230**, 104–110.
16. Kirimura K, Gunji H, Wakayama R, Hattori T & Ishii Y (2010). Enzymatic Kolbe–Schmitt reaction to form salicylic acid from phenol: Enzymatic characterization and gene identification of a novel enzyme, *Trichosporon moniliiforme* salicylic acid decarboxylase. *Biochem. Biophys. Res. Comm.* **394**, 279–284.
17. Yoshida T, Hayakawa Y, Matsui T & Nagasawa T (2004). Purification and characterization of 2,6-dihydroxybenzoate decarboxylase reversibly catalyzing nonoxidative decarboxylation. *Arch. Microbiol.* **181**, 391–397.

18. Wuensch C, Gross J, Steinkellner G, Lyskowski A, Gruber K, Glueck SM & Faber K (2014). Regioselective ortho-carboxylation of phenols catalyzed by benzoic acid decarboxylases: a biocatalytic equivalent to the Kolbe–Schmitt reaction. *RSC Adv.* **4**, 9673–9679.
19. Wieser M, Fujii N, Yoshida T & Nagasawa T (1998). Carbon dioxide fixation by reversible pyrrole-2-carboxylate decarboxylase from *Bacillus megaterium* PYR2910. *Eur. J. Biochem.* **257**, 495–499.
20. Ramsden CA, Riley PA (2014). Tyrosinase: the four oxidation states of the active site and their relevance to enzymatic activation, oxidation and inactivation. *Bioorg. Med. Chem.* **22**, 2388–2395.
21. Ienaga S, Kosaka S, Honda Y, Ishii Y & Kirimura K (2013). p-Aminosalicylic Acid Production by Enzymatic Kolbe-Schmitt Reaction Using Salicylic Acid Decarboxylases Improved through Site-Directed Mutagenesis. *Bull. Chem. Soc. Jpn.* **86**, 628–634.
22. Selwyn MJ (1954). A simple test for inactivation of an enzyme during assay. *Biochim. Biophys. Acta* **105**, 193–195.
23. Pierpont CG & Lange CW (1994). The Chemistry of Transition Metal Complexes Containing Catechol and Semiquinone Ligands. *Progr. Inorg. Chem.* **41**, 331–442.
24. Markovic Z, Engelbrecht JP & Markovic S (2002). Theoretical study of the Kolbe-Schmitt reaction mechanism. *Z. Naturforsch A Phys Sci* **57**, 812–818.
25. Matsuda T, Ohashi Y, Harada T, Yanagihara R, Nagasawa T & Nakamura K (2001). Conversion of pyrrole to pyrrole-2-carboxylate by cells of *Bacillus megaterium* in supercritical CO<sub>2</sub>. *Chem. Commun.*, 2194–2195.
26. Hofland GW, Rijke A de, Thiering R, van der Wielen, Luuk A.M & Witkamp G (2000). Isoelectric precipitation of soybean protein using carbon dioxide as a volatile acid. *J. Chromatogr. B* **743**, 357–368.
27. Bamberger A, Sieder G & Maurer G (2000). High-pressure (vapor+liquid) equilibrium in binary mixtures of (carbon dioxide+water or acetic acid) at temperatures from 313 to 353 K. *J. Supercrit. Fluids* **17**, 97–110.
28. Dodds WS, Stutzman LF & Sollami BJ (1956). Carbon Dioxide Solubility in Water. *Ind. Eng. Chem. Chem. Eng. Data Series* **1**, 92–95.
29. Jaenicke R (1981). Enzymes under extremes of physical conditions. *Ann. Rev. Biophys. Bioeng.* **10**, 1–67.
30. Brummund J, Meyer F, Liese A, Eggers R & Hilterhaus L (2011). Dissolving carbon dioxide in high viscous substrates to accelerate biocatalytic reactions. *Biotechnol. Bioeng.* **108**, 2765–2769.
31. Gerhard M & Schomburg D (2013) Biochemical pathways: an atlas of biochemistry and molecular biology 2nd edition, John Wiley and sons.
32. Everse J (1982) The Pyridine nucleotide coenzymes. Elsevier.



33. Santha R, Appaji Rao N & Vaidyanathan C (1996). Identification of the active-site peptide of 2,3-dihydroxybenzoic acid decarboxylase from *Aspergillus oryzae*. *Biochim. Biophys. Acta* **1293**, 191–200.
34. Schmidt ND, Peschon JJ & Segel IH (1983). Kinetics of enzymes subject to very strong product inhibition: Analysis using simplified integrated rate equations and average velocities. *J. Theor. Biol.* **100**, 597–611.
35. Hales JL, Jones JJ & Lindsey AS (1954). Mechanism of the Kolbe-Schmitt reaction. Part I. Infra-red studies. *J. Chem. Soc.*, 3145–3151.
36. Hirao I & Kito T (1973). Carboxylation of Phenol Derivatives. XXI. The Formation Reaction of the Complex from Alkali Phenoxide and Carbon Dioxide. *Bull. Chem. Soc. Jpn.* **46**, 3470–3474.
37. There is evidence that a part of potassium *p*-hydroxybenzoate is derived by rearrangement of initially formed  $K^+$  salicylate, while  $Na^+$  salicylate does not rearrange, see: Ota K (1974). The Conversion Reaction of Alkali 4-Hydroxyisophthalates into Hydroxybenzoic Acids. *Bull. Chem. Soc. Jpn.* **47**, 2343–2344.

## Tables

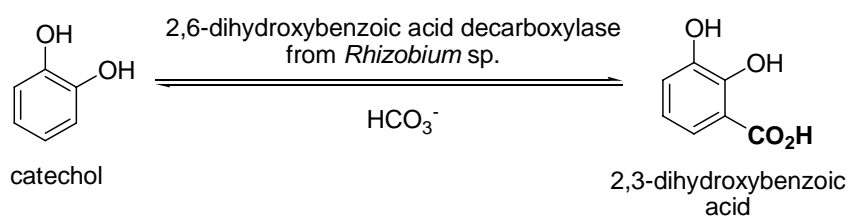
**Table 1. Catalytic parameters for enzymatic (de)carboxylation.**

Carboxylation					
$K_m$ (mM)		$V_{\max}^f$ ( $\mu\text{mol min}^{-1} \text{mg}^{-1}$ )	$k_{\text{cat}}$ ( $\text{s}^{-1}$ )	$K_a$ ( $\text{mM}^{-1} \text{s}^{-1}$ )	
catechol	bicarbonate	$0.35 \pm 1.1 \cdot 10^{-2}$	$0.12 \pm 3.0 \cdot 10^{-3}$	catechol	bicarbonate
$(K_{m,c})$	$(K_{m,b})$			$(K_a^c)$	$(K_a^b)$
$30 \pm 3$	$839 \pm 4$			$4.2 \cdot 10^{-3} \pm$	$1.5 \cdot 10^{-4} \pm$
				$6.5 \cdot 10^{-4}$	$5.7 \cdot 10^{-6}$
Decarboxylation					
$K_m$ (mM)		$V_{\max}^r$ ( $\mu\text{mol min}^{-1} \text{mg}^{-1}$ )	$k_{\text{cat}}$ ( $\text{s}^{-1}$ )	$K_a^{\text{HA}}$ ( $\text{mM}^{-1} \text{s}^{-1}$ )	
DHBA ( $K_{m,\text{HA}}$ )		$1 \pm 0.1$	$0.52 \pm 0.025$	$0.44 \pm 9 \cdot 10^{-2}$	
$1.2 \pm 0.3$					

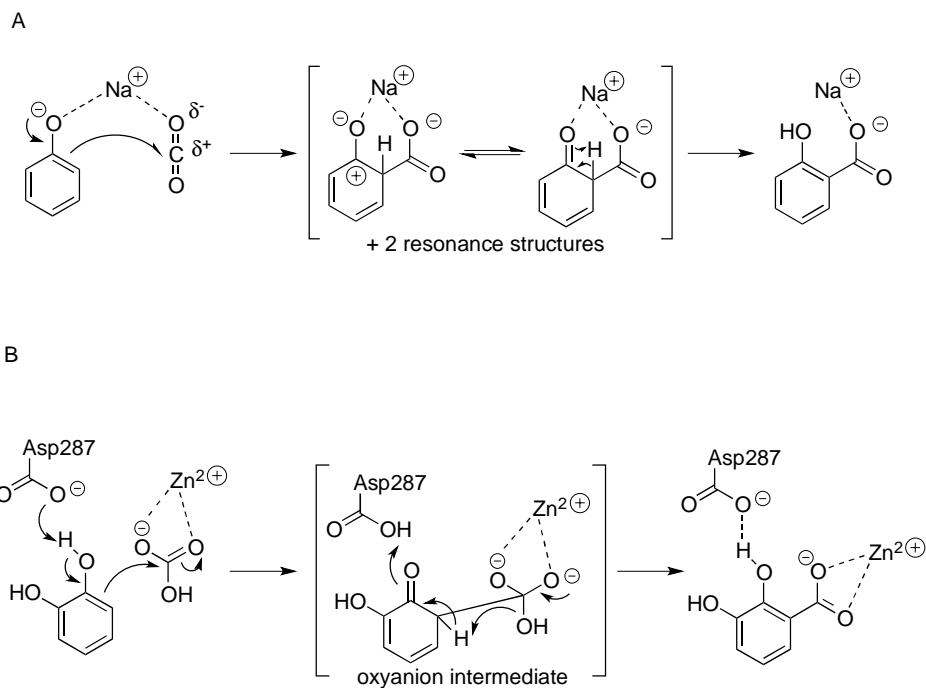
**Table 2. Carboxylation under CO<sub>2</sub> pressure.** Reactions were performed using 10 mM of catechol and 10 mM of ascorbic acid in KP<sub>i</sub> buffer (0.2 M pH 8.0) for 24h at 40 °C and 500 rpm.

CO <sub>2</sub> pressure (bar)	Max. conversion (%)
50	5
80	7
80, KHCO <sub>3</sub> (2M)	25

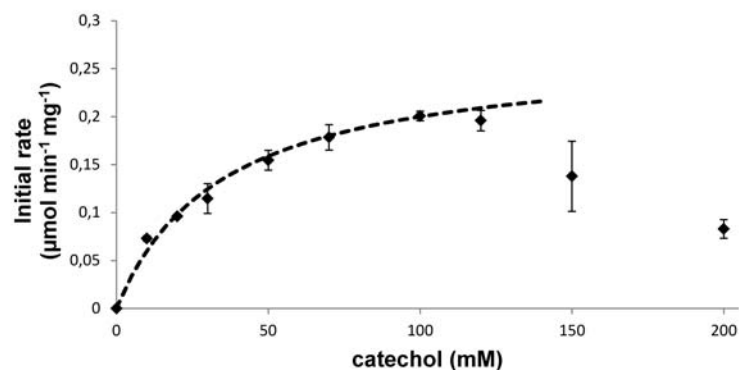
#### Schema



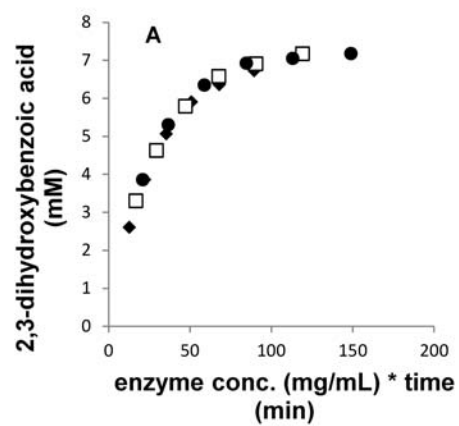
**Scheme 1. Enzymatic carboxylation (forward) and decarboxylation (reverse reaction) of catechol catalyzed by DHBA decarboxylase using bicarbonate as CO<sub>2</sub> source.**

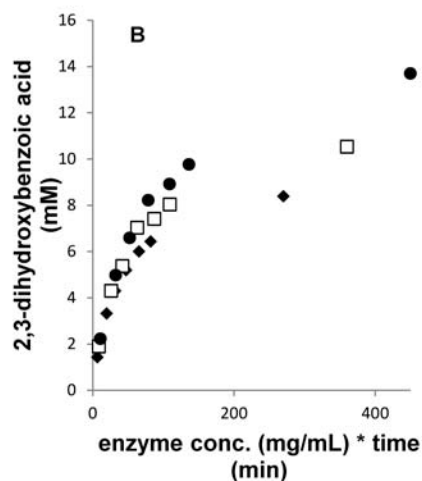


**Scheme 2. Comparison of the key steps in the mechanism of the chemical (A) and biological (B) Kolbe-Schmitt reaction.**

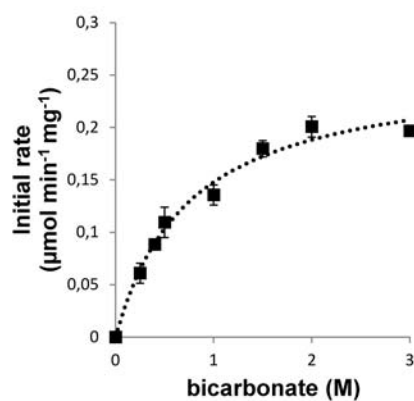


**Fig. 1. Initial rate measurements from carboxylation of catechol and Michaelis-Menten non-linear fit.** Reactions were performed using different catechol concentrations and stoichiometric amounts of ascorbic acid, 2 M KHCO<sub>3</sub>, 0.2-0.3 mg/mL of decarboxylase, at 30°C and 500 rpm. Dotted line: non-linear fit using the double substrate Michaelis-Menten model.



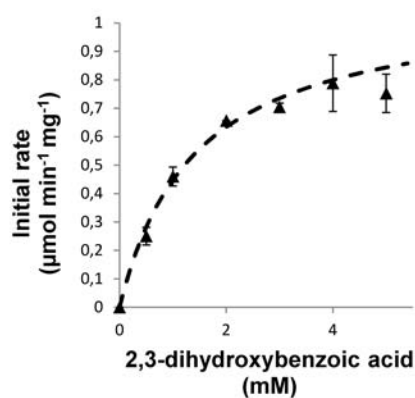


**Fig. 2. Deactivation test.** Progress curves obtained with varying amounts of DHBA decarboxylase CFE at fixed catechol concentrations of 30 mM (A) and 200 mM (B); black diamonds: 60 µL (0.21 mg/mL), white squares: 80 µL (0.28 mg/mL), black circles: 100 µL (0.35 mg/mL). The reactions were performed using 2 M of  $\text{KHCO}_3$  at 30°C and 500 rpm.

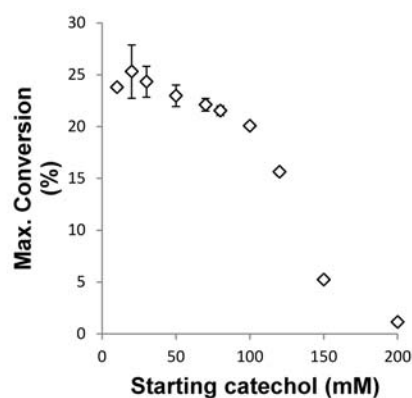


**Fig. 3. Michaelis-Menten non-linear fit for hydrogen carbonate in the carboxylation of catechol.** Reactions were performed at varying  $\text{KHCO}_3$  concentrations using 100 mM of catechol, 0.3-0.4 mg/mL of decarboxylase at 30°C and 500 rpm. Dotted line: non-linear fit using double substrate Michaelis-Menten model.

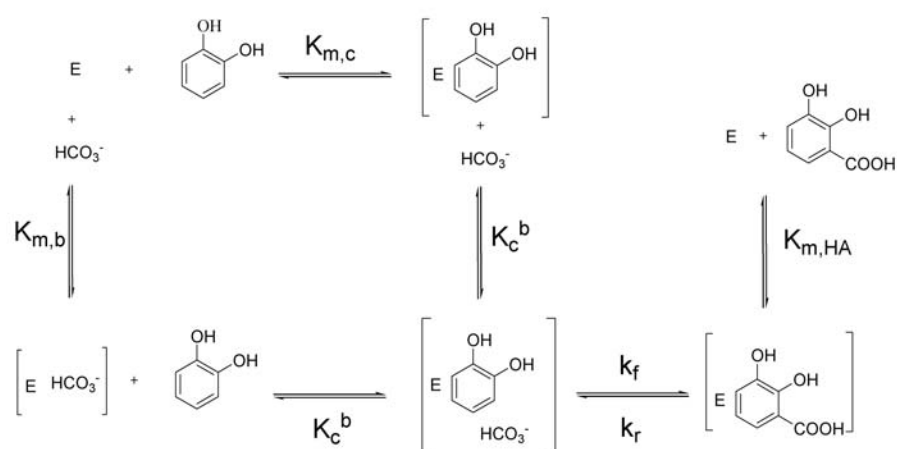




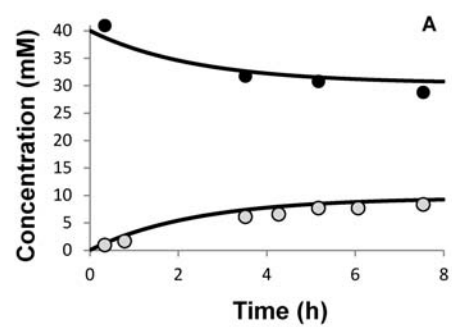
**Fig. 4. Michaelis-Menten non-linear fit for the decarboxylation of 2,3-dihydroxybenzoic acid.** Reactions were performed using various concentrations of DHBA,  $\text{KP}_i$  buffer 0.1 M at pH 8.0, 0.2-0.3 mg/mL of decarboxylase, and equimolar amounts of ascorbic acid at 30°C and 500 rpm. Dotted line: non-linear fit using single substrate Michaelis-Menten model.

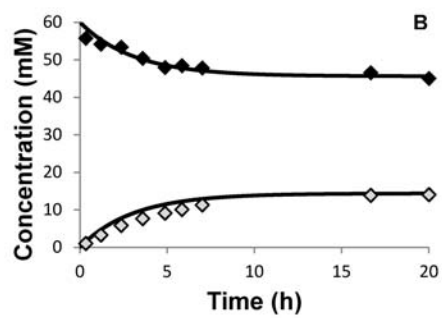


**Fig. 5. Long-term experiments at fixed bicarbonate and varying catechol concentrations.** Reactions were performed at 30°C, 500 rpm in the presence of 2 M of  $\text{KHCO}_3$  with varying catechol concentration, decarboxylase concentrations ranging from 0.5 to 1 mg/mL.



**Fig. 6. Kinetic equation and catalytic steps for a rapid equilibrium random and reversible bi-uni mechanism for biocatalytic carboxylation.** HA: 2,3-dihydroxybenzoic acid; E: enzyme = DHBA decarboxylase; C: substrate catechol; B: co-substrate bicarbonate;  $V_{\max}^f$ : maximum rate in carboxylation (forward) direction;  $V_{\max}^r$ : maximum rate in decarboxylation (reverse) direction;  $K_{m,c}$ : Michaelis constant for catechol;  $K_{m,b}$ : Michaelis constant for bicarbonate;  $K_{m,HA}$ : Michaelis constant for 2,3-dihydroxybenzoic acid;  $K_c^b$ : dissociation constant of ternary enzyme-two-substrate complex;  $k_f = k_{cat}$  in forward direction;  $k_r = k_{cat}$  in reverse direction





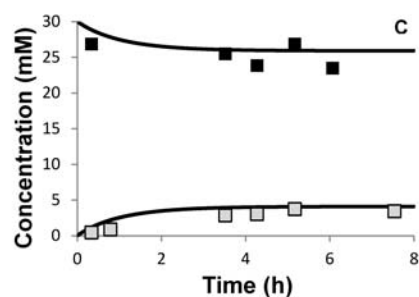


**Fig. 7. Simulation of batch reactions and comparison with experimental data.** Continuous lines result from simulation. A: catechol 40 mM,  $\text{KHCO}_3$  2 M, DHBA decarboxylase 0.22 mg/mL; B: catechol 60 mM,  $\text{KHCO}_3$  2 M, decarboxylase 0.25 mg/mL; C: catechol 30 mM,  $\text{KHCO}_3$  1 M, decarboxylase 0.25 mg/mL.



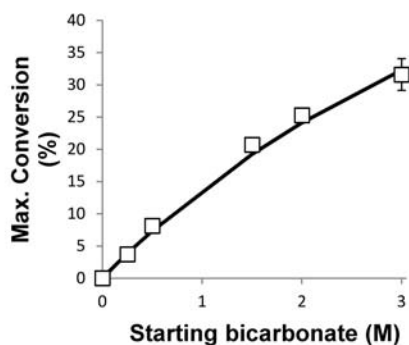


**Fig. 8. Comparison of experimental (white rectangles) and simulated (black line) equilibrium conversions.** Reactions were performed at 30°C, 500 rpm in the presence of 10 mM of catechol with various  $\text{KHCO}_3$  starting concentrations and decarboxylase concentrations ranging from 0.5 to 1 mg/mL.